

3

3-APTMS and tetrahydrofuranhydroperoxide mediated synthesis of AuNPs: Application in glutathione sensing

3.1. INTRODUCTION

Functionalization of noble metal nanoparticles with a wide range of organic or biological ligands has received wide attention for the selective binding and detection of small molecules and biological targets (Daniel and Astruc, 2004; Haick, 2007; Zayats et al., 2005; Radwan and Azzazy, 2009). Functionality in metal nanoparticles is important in determining its application for various practical purposes. Many reports are available where functionality has played a vital role (Evans et al., 2000; Zhang et al., 2002; Jeong et al., 2013). In addition to that the size of these nanomaterials has remarkable influence on the binding events enabling the development of innovative technological designs (Zamborini et al., 2002). Accordingly, the synthesis of nanoparticles displaying tunable functionality and nanogeometry has been a challenging requirement. Nanomaterials functionalized/stabilized through amino groups have received close attention due to their ubiquitous nature especially in biological and environmental systems as such functionality enable biocompatible linkage (Mirzabekov et al., 2000; Xu et al., 2004). Gold nanoparticles are

being tested for their use in cancer therapy as drug carriers, photothermal agents, contrast agents and radiosensitizers (Jain et al., 2012). Organically-soluble gold nanocrystals passivated with alkylamines have shown chemical and physical characteristics consistent with charge-neutral amine/gold surface interactions described by weak covalent bonds. Amines form only weakly bound and chemically unstable monolayers on bulk Au surfaces. In contrast, the amine-capped nanocrystals are nearly as stable as their thiol-capped counterparts (Leff et al., 1996). Apart from this functional activity of organic amine, a large number of reports show their stabilizing and reducing ability for noble metal salts (Liu et al., 2007; Bhargava et al., 2005; Aslam et al., 2004). Newman et al. (2006) reported the ability of various amines as reducing and stabilizing agents useful in the formation of AuNPs based on Marcus electron transfer theory. Zhu et al. (2005) have reported very slow conversion to nanoparticles when 3-APTMS and trimethoxysilylpropyl ethylenediamine were used. These findings reveal the reducing and stabilizing ability of 3-APTMS but predict the requirement of additional reducing agent for rapid and controlled nanoparticle synthesis. 3-GPTMS efficiently facilitate the reduction of Pd²⁺ ions, demonstrating the opening of epoxide ring of 3-GPTMS by Lewis acid character of palladium chloride (Pandey et al., 2001b). Such functional ability of 3-APTMS and 3-GPTMS has subsequently been examined on the controlled synthesis of AuNPs, AgNPs and PdNPs from respective noble metal salts (Pandey and Chauhan, 2012). The dispersibility of AuNPs in aqueous and organic solvents depends on the concentration of 3-APTMS and 3-GPTMS that has been used during the synthesis as discussed in previous chapter. But, the use of two alkoxysilanes of optimum concentrations led to the silanol group hydrolysis to form Si–O–Si linkage, hence, posing a problem in use of these materials for many required practical purposes. Accordingly, substitute of 3-GPTMS by other suitable biocompatible

organic reagents is sought. Tetrahydrofuran hydroperoxide (THF-HPO) along with 3-APTMS has been found to be a better option which not only reduced the silane content but also expedited nanoparticle formation with an additional advantage of producing biocompatible reaction product. The choice of these reagents during noble metal nanoparticles synthesis enabled control over size as a function of 3-APTMS concentration, even after the synthesis of nanoparticles, and as a function of THF-HPO concentration at constant concentrations of 3-APTMS. The finding justifying concentration dependent tuning of functional activity and nanogeometry, which has been a challenging requirement in the area of nanoparticle synthesis, is reported in the present chapter.

Glutathione (GSH) is a biologically important molecule and has specific interaction with hydrogen peroxide, H_2O_2 (Ma et al., 2012). Such specific interaction has been manipulated by the use of nanomaterials for precise GSH sensing (Xian et al., 2013; Hong et al., 2006). Accordingly, functional noble metal nanoparticles like AuNPs may provide valuable information on GSH sensing and the role of functionality could be manipulated based on differential catalytic ability of 3-APTMS-functionalized AuNPs. Fortunately, an interesting finding is recorded while monitoring the AuNPs-dependent catalysis of o-dianisidine in the presence of H_2O_2 as a function of GSH concentration. The AuNPs catalytic oxidation of o-dianisidine has also been found to vary as a function of 3-APTMS concentrations of as synthesized AuNPs representing the first report on the role of functionality of AuNPs in chemical sensing. In addition, a comparison on the catalytic efficiency of AuNPs in GSH sensing as a function of functionality and nanogeometry has also been demonstrated.

3.2. EXPERIMENTAL

3.2.1. Materials and instrumentation

The following chemicals are used: 3-Aminopropyltrimethoxysilane is obtained from Aldrich Chem. Co.; tetrachloroauric acid, is purchased from HiMedia; hydrogen peroxide, glutathione are obtained from Merck, India and o-dianisidine from Loba Chemie. All other chemicals employed were of analytical grade. Aqueous solutions were prepared by using doubly distilled-deionized water (Elga water purification system).

3.2.2. Synthesis of functional AuNPs

3.2.2.1. 3-APTMS and THF-HPO mediated AuNPs synthesis

The typical process for AuNPs synthesis involves the mixing of an aqueous solution of metal salts and 3-APTMS at a desired ratio (Table 3.1). The 3-APTMS treated metal salt was then allowed to interact with THF-HPO. Synthesis of AuNPs was observed under the following two conditions: (1) varying 3-APTMS (Table 3.1, sample no. i–vi) at constant concentration of THF-HPO and, (2) varying THF-HPO (Table 3.1, sample no. vii–xiii, iv and vi) and keeping the concentration of 3-APTMS constant. A typical THFHPO and 3-APTMS mediated synthesis of AuNPs sol was conducted as follows: 50 μ L of 10 mM of HAuCl₄ solution in water was premixed with 40 μ L aqueous solution of 3-APTMS stirred for 2 min, followed by addition of THF-HPO. The volume was made up to 2 mL with water in each case. The solution was kept undisturbed in the dark for 30 min. AuNPs sols of red/purple/blue color were obtained within <30 min indicating the formation of different sizes of AuNPs.

3.2.2.2. 3-APTMS and GBL mediated AuNPs synthesis

50 μ L of 10 mM of HAuCl₄ solution in water was premixed with varying concentrations of 40 μ L aqueous solution of 3-APTMS (sample no. xiv–xvi, Table 3.2) stirred for 2 min, followed by addition of varying GBL concentration (sample no. xvii–xix, Table 3.2). The volume was made up to 130 μ L in each case. The solution was kept undisturbed in the dark for 3–4 h.

Table 3.1. 3-APTMS and THF-HPO mediated synthesis of AuNPs showing change in λ_{max} as a function of reactant concentrations

Sample No.	3-APTMS (mM)	THF-HPO (mg)	λ_{max} (nm)
i	4.0	11.3	526
ii	6.0	11.3	530
iii	8.0	11.3	532
iv	10.0	11.3	553
v	12.0	11.3	565
vi	14.0	11.3	569
vii	5.0	11.3	523
viii	5.0	33.9	519
ix	5.0	56.5	519
x	10.0	33.9	524
xi	10.0	56.5	524
xii	14.0	33.9	536
xiii	14.0	56.5	536

3.2.3. Peroxidase-like catalytic activity of AuNPs made using 3-APTMS and THF-HPO

The peroxidase like activity of as synthesized AuNPs was determined spectrophotometrically by measuring the formation of oxidized product of o-dianisidine at 430 nm ($\epsilon=11.3 \text{ mM}^{-1}\text{cm}^{-1}$) using a Hitachi U-2900 spectrophotometer. O-dianisidine is a peroxidase substrate which in the presence of enzyme and H_2O_2 gives peak at $\sim 430\text{nm}$ corresponding to oxidized o-dianisidine. Typically, the o-dianisidine oxidation activity was measured in water using o-dianisidine at 25°C . In brief, $40\mu\text{L}$ of $3.2 \text{ M H}_2\text{O}_2$, $70\mu\text{L}$ of 10mM o-dianisidine, and $200\mu\text{L}$ of AuNPs were added into $500.0 \mu\text{L}$ of water and then the solution was mixed up to make it uniform and spectra for the three shades was recorded at fixed time intervals.

Table 3.2. Effect of GBL on 3-APTMS-mediated synthesis of AuNPs

Sample No.	3-APTMS (mM)	GBL (mg)	λ_{max} (nm)
xiv	5	40	531
xv	7	40	558
xvi	10	40	579
xvii	5	50	537
xviii	5	60	545
xix	5	70	571

3.2.4. Glutathione detection by measuring wastage of H_2O_2

As explained above o-dianisidine in the presence of AuNPs and H_2O_2 gives peak at around 430nm . However, when GSH is added to the system it competes with o-dianisidine for

H₂O₂ as GSH forms dimer on reacting with H₂O₂. Thus, by measuring the amount of H₂O₂ that is getting wasted in forming dimer with GSH gives the measure of GSH. The GSH samples were detected according to the following steps: 40µL of 3.2 M H₂O₂, 25µL of different concentrations of GSH, 70µL of 10 mM o-dianisidine and 200 µL of synthesized AuNPs were added into 500µL of water. After incubating for 75 min, the measurement was started. The absorbance change was monitored at 430 nm. The final concentrations of GSH in the system varied from 24.5µM to 172µM.

3.2.5. Kinetic Parameter Analysis

The steady-state kinetics were performed by varying the concentration of H₂O₂ (58.9 mM–980mM), at fixed concentration of o-dianisidine (344.0 mM). The reaction was carried out in 2 mL water and the variation of absorbance was monitored using a spectrophotometer (Hitachi U-2900) in time scan mode at 430 nm ($\epsilon=11.3 \text{ mM}^{-1}\text{cm}^{-1}$). The kinetic parameters were calculated by fitting the absorbance data to Michaelis–Menten equation as,

$$v=V_{\max}[C]/K_m + [C]$$

Where v is the initial velocity, V_{\max} is the maximal reaction velocity, C is the concentration of the substrate, and K_m is the Michaelis–Menten constant.

3.3. RESULTS

3.3.1. 3-APTMS and THF-HPO mediated AuNPs

3-APTMS and 3-GPTMS mediated synthesis of AuNPs having dispersibility in aqueous media under specific concentration of 3-APTMS and 3-GPTMS and in non-aqueous media at all concentrations of the same, was reported in chapter 2. Such findings although

provided a report on the synthesis of AuNPs, but suffered a disadvantage due to increased alkoxy silane content which limits its use for many practical applications due to the formation of Si–O–Si linkage with time. Accordingly, an attempt has been made in the present chapter to decrease the silane content by substituting some other reagent in place of alkoxy silanes. Since, 3-APTMS acts not only as reducer but also as a potential stabilizer, potential substitute of 3-GPTMS is sought. Fortunately, THF-HPO provided valuable information on the synthesis that not only decreased the silane content but also expedited the controlled formation of AuNPs. THF-HPO used was readily available by the autooxidation of tetrahydrofuran (Rein and Creigee, 1950). The detailed investigation on the synthesis of AuNPs is discussed herein. In the first instance, the role of 3-APTMS and THF-HPO in reducing Au^{3+} and creating the stabilized nanoparticles was investigated. It is observed that the concentration-dependent participation of both 3-APTMS and THF-HPO are necessary for the rapid conversion of Au^{3+} into AuNPs. The conversion of constant concentration of chloroauric acid solution (0.625 mM) into AuNPs is examined under two different conditions: (i) varying 3-APTMS while keeping THFHPO concentration constant (Fig. 3.1), and (ii) varying the THFHPO while keeping 3-APTMS concentration constant. To observe the effect of THF-HPO three different concentrations of 3-APTMS were selected (a) 5mM (Fig. 3.2); (b) 10mM (Fig.3.3); and (c) 14mM (Fig. 3.4). The concentrations of 3-APTMS and THF-HPO required during AuNPs synthesis are given in Table 3.1. There is a well established relationship between AuNPs size and plasmon band position, with the plasmon resonance band shifting to the red and broadening with increasing particle size (Aslam et al., 2004). From the UV-Vis spectroscopy study as given in Fig. 3.1, it can be observed that the peak shifts towards red region with increasing concentration of 3-APTMS which means AuNPs size is increasing, while in the case of

increasing THF-HPO concentration at constant 3-APTMS as given in Fig. 3.2 - Fig. 3.4 peak shifts towards blue region indicating a decrease in the size of AuNPs with increasing THF-HPO concentration.

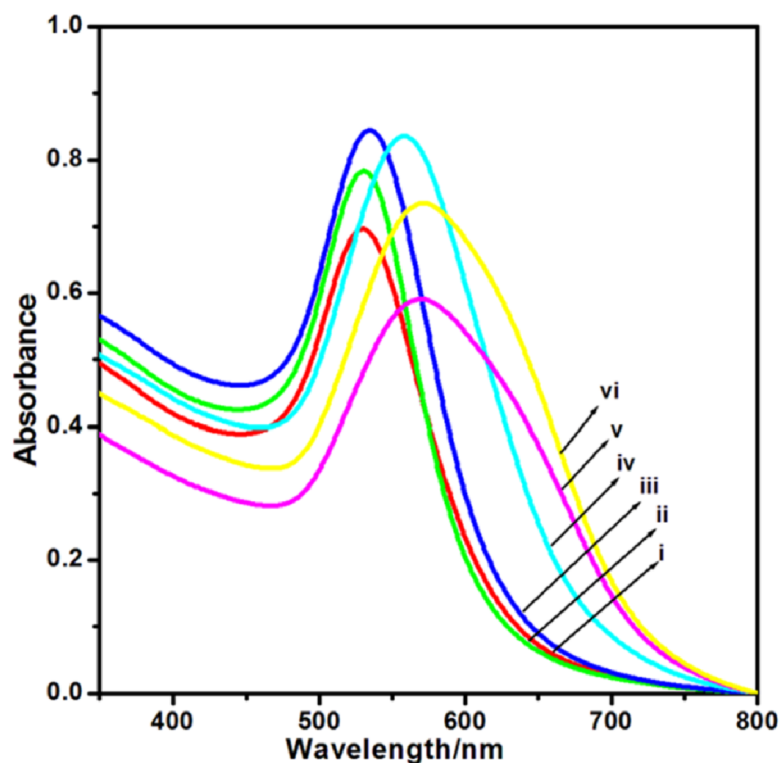


Figure 3.1. UV-Vis spectra showing change in λ_{\max} of AuNPs made using constant concentration of THF-HPO (11.3 mg) and varying concentrations of 3-APTMS; (i) 4mM, (ii) 6mM, (iii) 8mM, (iv) 10mM, (v) 12mM, and (vi) 14mM.

Thus, there exists flexibility in synthetic route and the size of AuNPs can be decreased even at high 3-APTMS concentration by addition of THF-HPO and size can be increased by increasing 3-APTMS at constant concentration of THF-HPO. This flexibility in synthesis route has been utilized to justify the role of both nanogeometry and amino functionality in chemical sensing and is discussed later. The TEM images of AuNPs made using different 3-APTMS concentration at constant concentration of THF-HPO are given

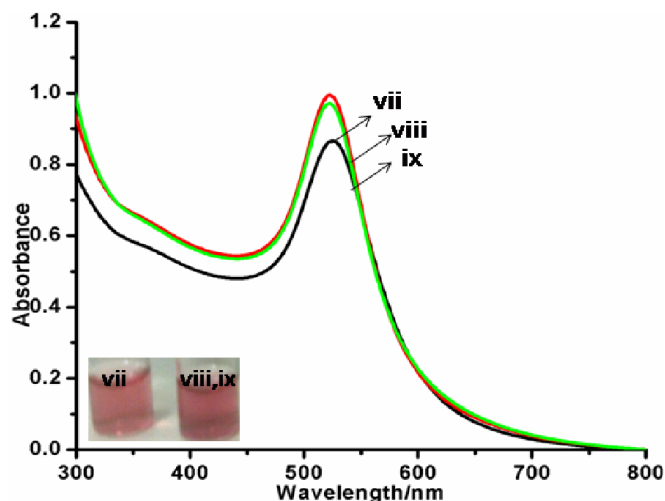


Figure 3.2. UV-Vis spectra showing change in λ_{\max} of AuNPs made using 3-APTMS (A=5mM) containing THF-HPO of three different concentrations [11.3 mg (black line, vii), 33.9 mg (red line, viii) and 56.5 mg (green line, ix)].

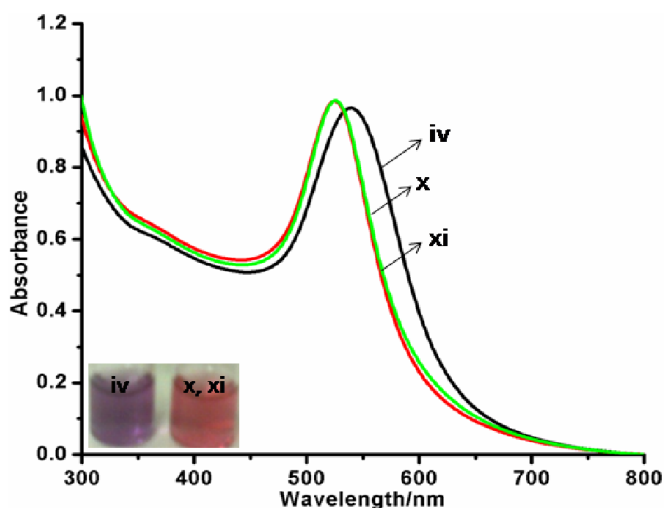


Figure 3.3. UV-Vis spectra showing change in λ_{\max} of AuNPs made using 3-APTMS (A=10mM) containing THF-HPO of three different concentrations [11.3 mg (black line, iv), 33.9 mg (red line, x) and 56.5 mg (green line, xi)].

in Fig. 3.5. The variation of λ_{\max} as shown in Table 3.1 suggest the choice of 3-APTMS concentrations corresponding to 4mM, 10mM and 14mM at constant concentration of

THF-HPO (11.3 mg) yielding reasonable difference in size of AuNPs with λ_{\max} at 530 nm, 558 nm and 571 nm.

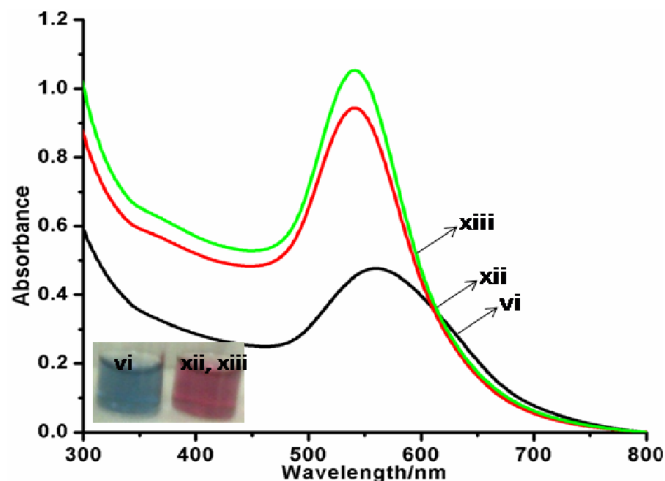


Figure 3.4. UV-Vis spectra showing change in λ_{\max} of AuNPs made using 3-APTMS (A=14mM) containing THF-HPO of three different concentrations [11.3 mg (black line, vi), 33.9 mg (red line, xii) and 56.5 mg (green line, xiii)].

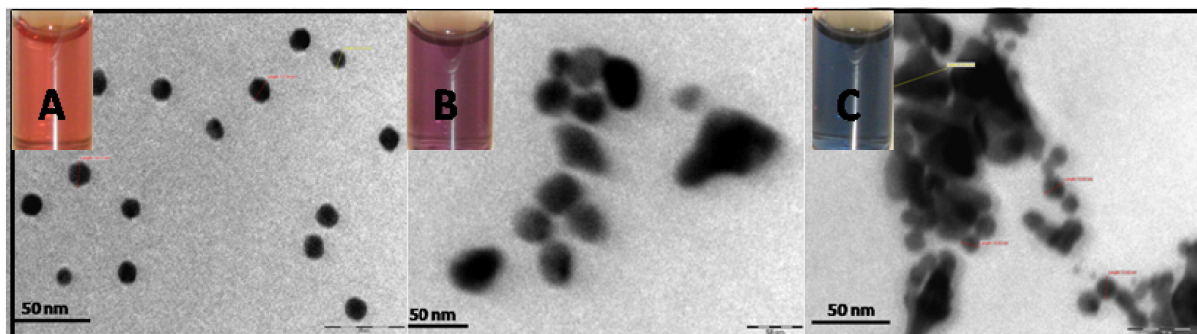


Figure 3.5. TEM images of AuNPs made from increasing concentrations of 3-APTMS (A= 4.0mM, B= 10mM and C= 14mM) containing constant concentration of THF-HPO (11.3 mg).

These AuNPs at a fixed concentration of 3-APTMS and THF-HPO gives a single persistent color which remains stable at room temperature for quite a long time thus enabling it to be used for various practical purposes.

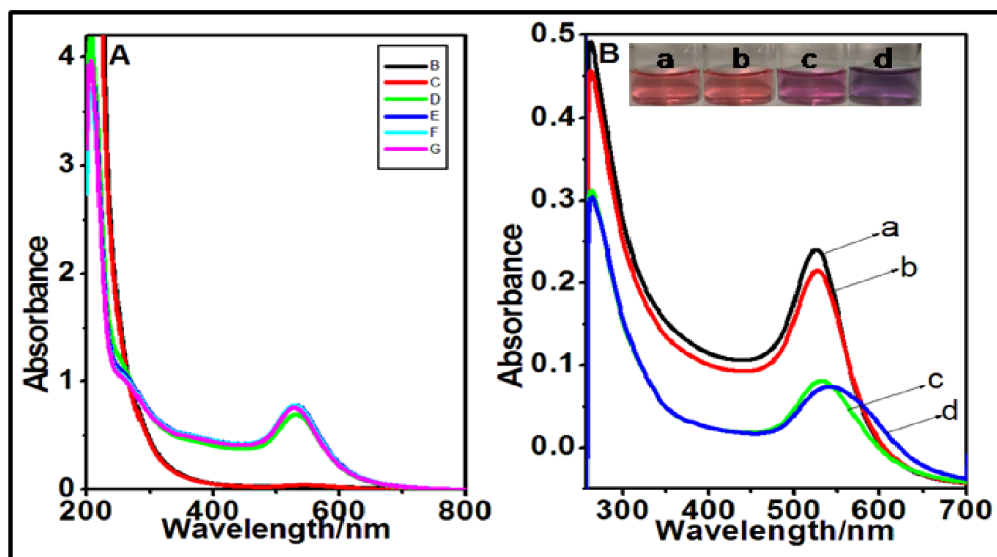


Figure 3.6. (A) Time dependent UV-Vis spectrum of AuNPs made using 3-APTMS (25 mM) and THF-HPO (11.3 mg), (B) change in λ_{\max} of same AuNPs (a) on the subsequent addition of 3-APTMS; 20mL; 50 mM (b),(c) and (d).

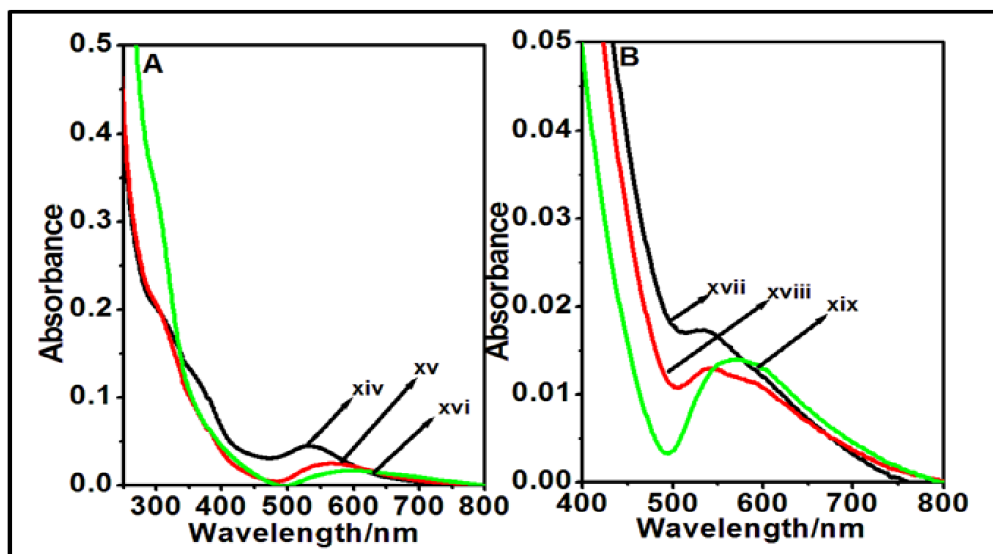


Figure 3.7. UV-Vis spectra of AuNPs made from GBL and 3-APTMS showing change in λ_{\max} as a function of: (A) variable concentrations of 3-APTMS (xvi=0.25 M, xv=0.35 M and xvi=0.5 M) with constant concentration of GBL (40 mg); (B) variable concentrations of GBL (xvii = 50.0 mg, xviii = 60 mg and xix = 70 mg) with constant concentration of 3-APTMS (0.25 M).

3.3.2. Chemistry of 3-APTMS and THF-HPO mediated AuNPs

After confirming the concentration-dependent role of THF-HPO and 3-APTMS on AuNPs synthesis, the mechanism of the process is investigated. To gain deeper insight into the mechanistic approach, the time dependent studies on the formation of AuNPs from 3-APTMS and THF-HPO have been attempted as shown in Fig. 3.6A. Figure revealed the occurrence of absorption peak at 210 nm that varies with time, suggesting the formation and consumption of the material, giving peak at 210nm, in due course. The peak at 210nm is due to formation of γ - butyrolactone (GBL) from THF-HPO as has been described later in the discussion section. The effect of subsequent addition of 3-APTMS into AuNPs after it has been synthesized has been given in Fig. 3.6B.

3.3.3. 3-APTMS and GBL mediated AuNPs: formation and consumption

Further, to explore the role of GBL during AuNPs synthesis, GBL was synthesized from THF (Leonid and Schmuell, 2000). The synthesized GBL was used further for AuNPs synthesis in place of THF-HPO. The nanoparticle formation with GBL in place of THF-HPO is not of much significance, as the nanoparticles formation took a comparatively long time with relatively little yield. Nevertheless, GBL also triggered the AuNPs synthesis in the presence 3-APTMS. Amino capped Au^{3+} ion was brought into contact with GBL (in place of THF-HPO) and was left undisturbed for 4–5 h under two different conditions; (i) varying 3-APTMS while keeping GBL concentration constant (Fig. 3.7A), and (ii) varying GBL (Fig. 3.7B) while keeping 3-APTMS concentration constant. Increased concentration of both the reactant (GBL/3-APTMS) increased the AuNPs size as shown in Table 3.2 and Fig. 3.7.

3.3.4. Effect of 3-APTMS concentration on catalytic property of AuNPs

Difference in sensory responses of nanoparticles based on their nanogeometry is much studied (Zhu et al., 2005) but the difference in sensory responses based on its functionality is still obscure. To investigate the enzyme mimetic activity of AuNPs the catalytic experiments were carried out using o-dianisidine as substrate. Upon the addition of AuNPs, the absorbance intensity of the o-dianisidine-H₂O₂ system increased due to the intrinsic peroxidase property of 3-APTMS functionalized AuNPs. The colorless o-dianisidine on reacting with H₂O₂ and AuNPs forms a brown colored product that can be read on spectrophotometer at ~430nm. First the effect of AuNPs size on its peroxidase like behavior was studied by observing the time dependent variation in the absorbance value of oxidized o-dianisidine (430nm) for three different sizes AuNPs. Three different sizes of AuNPs (35nm, 25nm and 10nm) were made by varying the 3-APTMS concentration as described in synthesis part. Fig. 3.8 gives the variation in λ_{max} value for o-dianisidine-H₂O₂-AuNPs system as a function of time for three different sizes of AuNPs (Fig. 3.8 A, B and C). The plot for the absorbance variation with time for AuNPs catalyzed o-dianisidine-H₂O₂ system as shown in Fig. 3.8D indicate that the large sized AuNPs are more active compared to small size of the AuNPs which is contrary to what is known through literature i.e. smaller the size more the catalysis. The K_m value for the largest AuNPs size, as it has been found to be most catalytic, has been calculated for the o-dianisidine-H₂O₂-AuNPs system by keeping the concentration of o-dianisidine constant and varying H₂O₂ concentration using same amount of AuNPs as catalyst (Fig.3.9).

The mimetic behavior of AuNPs has also been used for an interesting finding on colorimetric method for determination of GSH which is based on the competitive reaction of GSH and o-dianisidine with H_2O_2 in the presence of AuNPs.

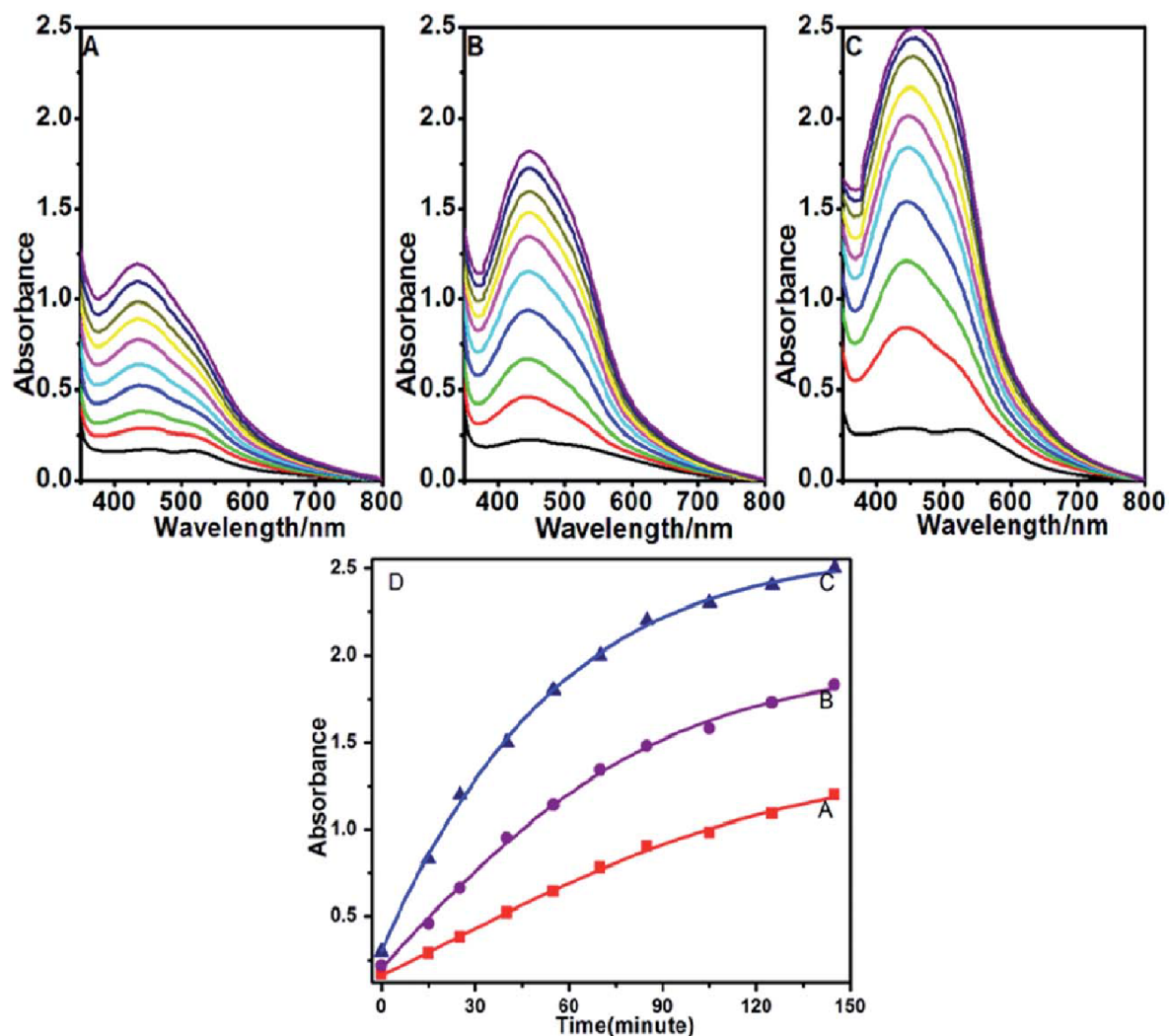


Figure 3.8. Time dependent UV-Vis spectral change of o-dianisidine-H₂O₂ system catalyzed by AuNPs of variable size; (A) 10 nm (B) 25 nm and (C) 35nm. Plot-D shows the time dependent variation of absorption at 430 nm calculated from plots A, B and C respectively.

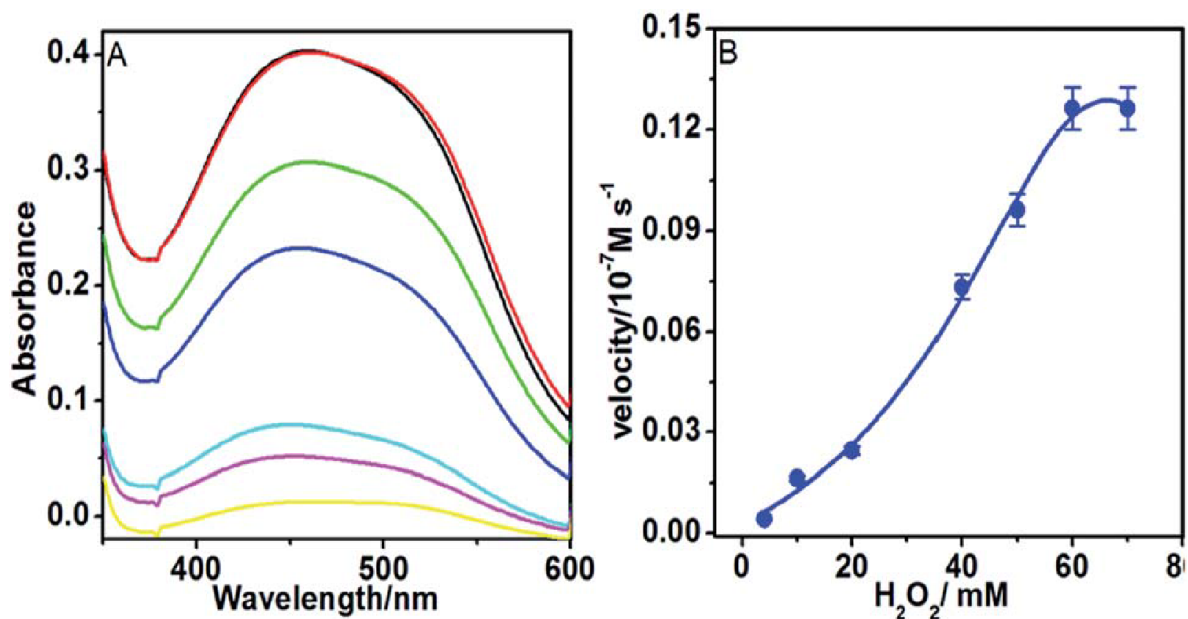


Figure 3.9. Kinetic analysis of o-dianisidine–AuNPs–H₂O₂ system with H₂O₂ as substrate. H₂O₂ concentration is varied from to 980mM–58.9 mM.

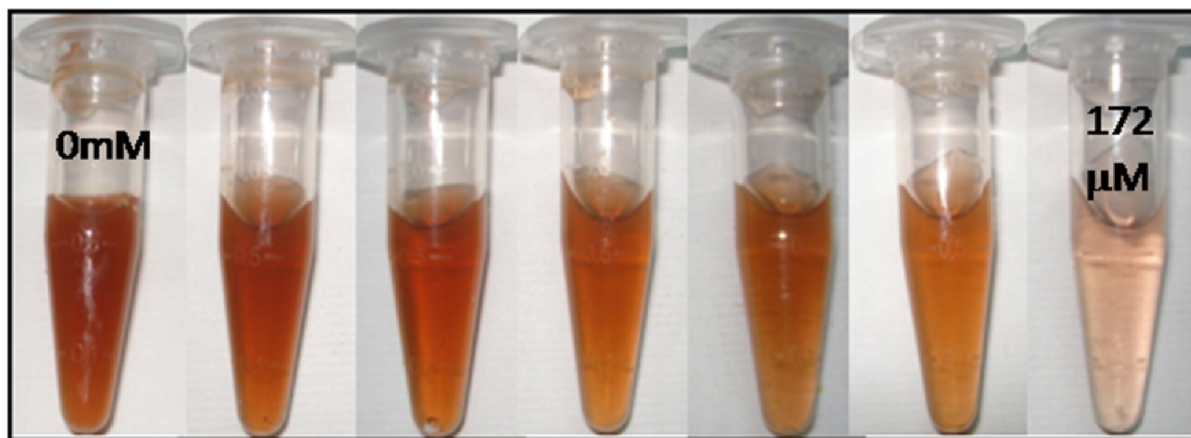


Figure 3.10. A typical photograph showing the effect of increasing concentration of glutathione on the intensity of the color, produced due to the oxidation of o-dianisidine in o-dianisidine-H₂O₂-AuNPs reaction system.

The comparison of three different sizes of AuNPs (10 nm, 25 nm and 35 nm) was made, again by recording the absorbance changes at fixed time that occur while catalyzing the oxidation of o-dianisidine in the presence of H₂O₂ at different GSH concentrations.

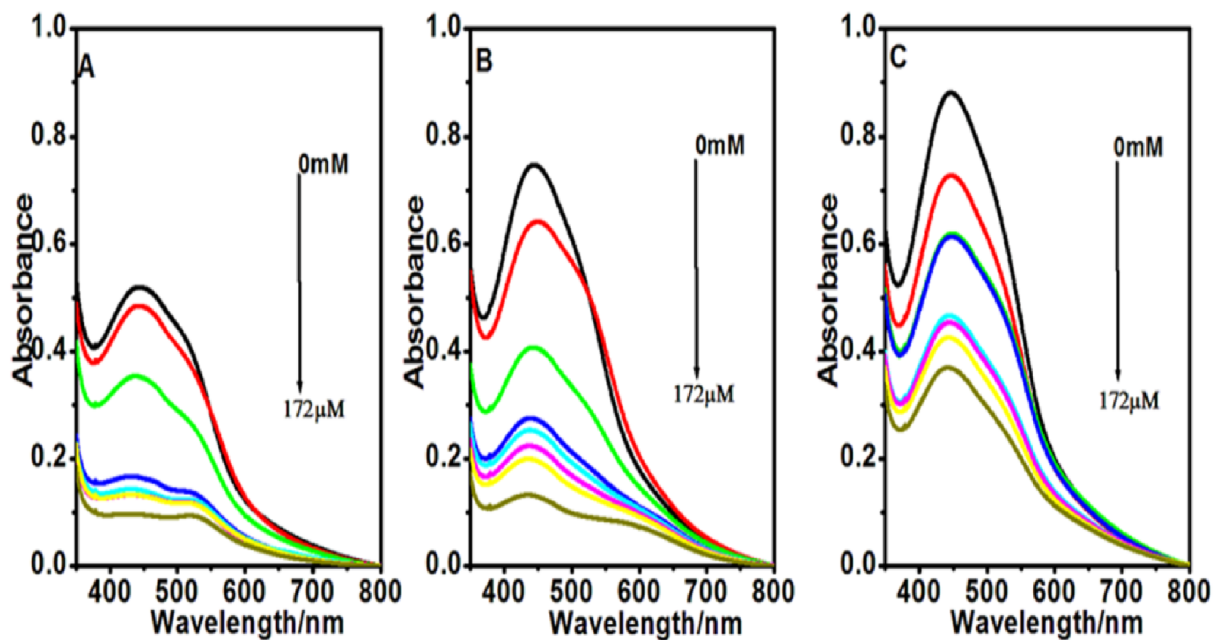


Figure 3.11. UV-Vis spectra of *o*-dianisidine–H₂O₂–AuNPs system in the presence of varying concentrations of GSH (0 mM–172 μM) for three sizes of AuNPs; (A) 10 nm (B) 25 nm (C) 35 nm; under the optimum conditions.

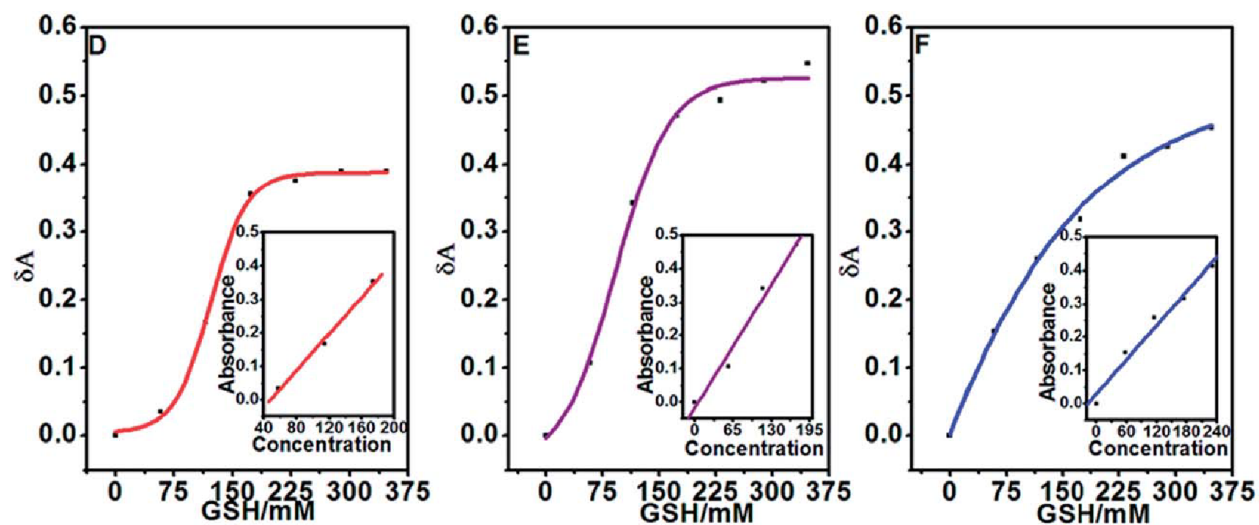


Figure 3.12. Response curves of GSH detection using *o*-dianisidine in the presence of AuNPs of three different sizes (D) 10 nm (E) 25 nm (F) 35 nm. Inset shows linear calibration plots for GSH analysis.

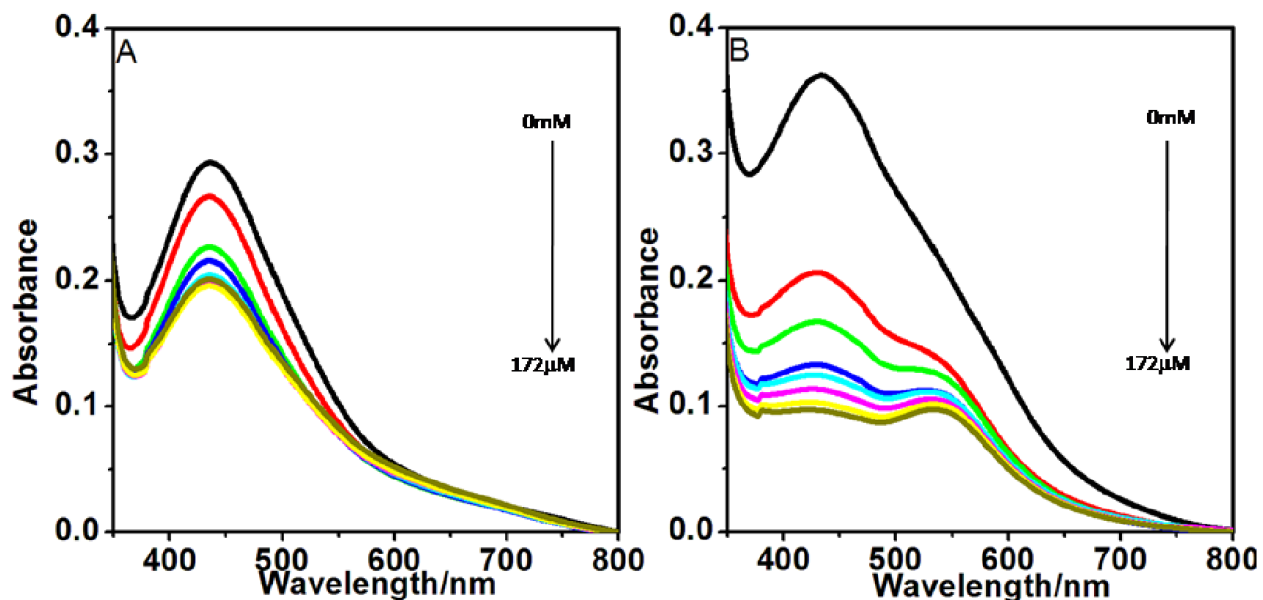


Figure 3.13. UV-Vis spectra of o-dianisidine–H₂O₂–AuNPs system in the presence of varying concentration of GSH (0 mM–172 mM). AuNPs of two size, (A= 35 nm, B=10 nm) were made at constant concentration of 3-APTMS (0.7).

Fig. 3.10 shows the variation in color of the oxidized o-dianisidine having same concentration of o-dianisidine and H₂O₂ but different (increasing) GSH concentration. Fig. 3.11 shows the relative absorbance-concentration plot for the three different sizes (35 nm, 25 nm and 10 nm). The linear range and detection limit as shown in Fig. 3.12 are found in the order AuNPs (35 nm) > AuNPs (25 nm) > AuNPs (10 nm).

From the results it can be deciphered that the catalysis observed is not only due to the AuNPs, and some other moiety is also responsible for the results obtained. From the work of Wight and Davis it is known that the imine linkage between 3-APTMS and carbonyl moiety is catalytic in nature. In the present case AuNPs size is increasing with increasing concentration of 3-APTMS and also imine linkage formed from 3-APTMS is catalytic in nature. So, the possibility is that 3-APTMS might be responsible for the unusual behavior

observed. To confirm one more comparison of catalytic behavior was made and this time 3-APTMS concentration was kept same and different sizes were obtained by varying THF-HPO amount. The results as shown in Fig. 3.13 clearly demonstrate that this time small sized AuNPs are more catalytic which means in case when 3-APTMS concentration is kept constant the AuNPs display size dependent catalysis.

3.4. DISCUSSION

3.4.1. Effect of 3-APTMS and THF-HPO on the AuNPs size

An increase in λ_{\max} with increasing 3-APTMS concentration (Table 3.1, system i–vi) and reverse for increasing THF-HPO (Table 3.1, system vii–xiii, iv and vi) was confirmed from the spectrophotometric analysis of the nanoparticles as shown in Fig. 3.1 and Fig. 3.2 - 3.4, respectively.

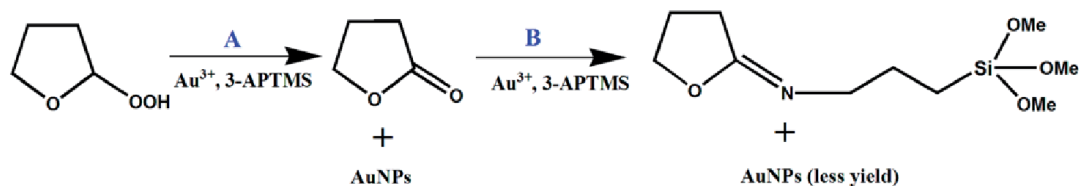
Thus, λ_{\max} values as given in Table 3.1 demonstrate that an increase in 3-APTMS concentration results in an increase in size of AuNPs, however, the same decreases on increasing the THF-HPO content (Table 3.1) (vii–ix, x–xi and xii–xiii). These findings predict the possibility of perfect control of nanogeometry based on fixed ratio of 3-APTMS/THF-HPO. TEM images of the AuNPs made at three different 3-APTMS concentration (4mM, 10mM and 14mM) as shown in Fig.3.5 also reveal that when the concentration of 3-APTMS increases from 4mM to 14mM the size of the nanoparticle increases from 10nm to 35nm. Thus, the more is the concentration of 3-APTMS, the larger is the size of resulting AuNPs. Further nanoparticles in Fig. 3.5A are well dispersed, symmetrical and its size is ~10 nm whereas the result shown in Fig.3.5B reveals agglomeration of nanoparticles leading to nanoparticle size of 25nm. The agglomeration

has further increased on increasing 3-APTMS to 14mM as shown in Fig. 3.5C resulting in nanoparticles of size 35 nm. Thus data on spectrophotometry and TEM images suggest an increase in nanoparticle size with increasing concentration of 3-APTMS. Further, TEM images also show agglomeration among AuNPs with increasing 3-APTMS concentration which is due to self assembling nature of 3-APTMS and this also proves the capping ability of 3-APTMS.

3.4.2. GBL mediated mechanism for the synthesis of AuNPs

Spectrophotometric monitoring of nanoparticle formation with time as shown in Fig.3.6A revealed the occurrence of absorption peak at 210 nm that could be due to the formation of GBL from THF-HPO since the formation of GBL from THF-HPO in the presence of metal ions is known (Murai et al., 1963) and GBL itself gives peak at around 210nm. Another hump at around 260 nm is observed during the course of study due to Au (AuNPs)–amine (3-APTMS) interaction. It can be seen from Fig. 3.6B that intensity of the peak corresponding to AuNPs decreases with subsequent increase in 3-APTMS concentration which is in sync with the decrease of peak around 260 nm. The λ_{\max} value for AuNPs increases with increasing 3-APTMS concentration enabling the conversion of small size AuNPs into larger size with subsequent reduction in the apparent number of AuNPs available for 3-APTMS interaction. Thus, it can be concluded that with increasing size or decreasing intensity of AuNPs there is decreased Au–amine interaction as can be seen from Fig. 3.6B. So, the peak around 260 nm can be designated to AuNPs– amine (3-APTMS) interaction. As can be inferred from Fig. 3.6B, there is a synchronized decrease in intensities of absorbance of the two peaks corresponding to 210 nm and 260 nm which means they are getting consumed together, that might result in imine derivative of GBL as

shown in Scheme 3.1. It can be deduced further from Fig. 3.6B that the peak at around 260 nm, corresponding to the AuNPs–amine (3-APTMS) interaction, also gets decreased with increasing 3-APTMS concentration. 3-APTMS though is a stabilizer but its increased concentration results in an increase in AuNPs size that could be due to its consumption (via route B, Scheme 3.1). Following important conclusions can be drawn from the experimental finding discussed above; (a) an increase in size of AuNPs with increasing 3-APTMS concentration, (b) decrease in size of AuNPs with increasing THF-HPO, (c) formation of GBL during the nanoparticle synthesis, (d) formation of peak at around 260 nm due to Au–amine interaction, (e) synchronized decrease in intensity of the peaks at 210 nm (GBL) and 260 nm (Au–amine) with time and, (f) decrease in intensity of the peak at 260 nm following subsequent addition of 3-APTMS accompanied with increased size of AuNPs. Based on these findings, the mechanism for 3-APTMS and THF-HPO mediated synthesis of AuNPs is proposed in Scheme 3.1.



Scheme 3.1. Mechanism of 3-APTMS and THF-HPO assisted synthesis of AuNPs.

Newman et al have studied in detail the reduction of Au^{3+} to Au^0 involving several amine compounds (Newmann and Blanchard, 2006). In our system Au^{3+} in the presence of THF-HPO and 3-APTMS gets reduced to form stabilized AuNPs accompanied by formation of GBL. The reduction of Au^{3+} to Au^0 is facilitated by THF-HPO oxidation to GBL. The resulting GBL in the presence of Au^{3+} and 3-APTMS may form imine derivative of GBL

under optimum conditions resulting again in the formation of AuNPs. Accordingly, the synthesis of AuNPs proceeds through reaction pathway A and B as shown in Scheme 3.1. At lower 3-APTMS concentration reaction mainly proceeds through pathway A, and at higher 3-APTMS pathway B comes into action as well. The nanoparticle synthesis using GBL and 3-APTMS as starting material has been shown in Fig. 3.7A and Fig. 3.7B and it has been observed that both have a kinetic role to play in imine formation. An increase in the concentration of either GBL or 3-APTMS resulted in increased size of AuNPs probably due to a decrease in 3-APTMS content associated with route B. At higher concentrations of 3-APTMS, the system also undergoes side reaction via route B, thus decreasing the 3-APTMS content and the resulting nanoparticles of increased size are formed which is also evident from the TEM images of nanoparticles. Route A results in nanoparticles of smaller size, whereas route-B results in nanoparticles of higher size. This explains the higher nanogeometry with increasing 3-APTMS. The size of the synthesized AuNPs can further be manipulated by adding 3-APTMS to the synthesized AuNPs.

3.4.3. Role of nanogeometry and functionality in chemical sensing

The use of AuNPs in place of peroxidase enzyme to catalyze o-dianisidine- H_2O_2 system is shown in Fig. 3.8. The results also demonstrate that the AuNPs made at higher 3-APTMS concentration (35 nm) shows better catalytic property as compared to that made at lower concentrations of the same (25 and 15 nm). The peroxidase-like catalytic property for the fastest system (AuNPs size = 35 nm) was further investigated using steady-state kinetics. The kinetic data were obtained by varying H_2O_2 concentration while keeping the other substrate concentrations constant as shown in Fig. 3.9. The kinetic analysis of o-dianisidine-AuNPs system at varying H_2O_2 concentrations gave K_m value of 38.12 mM.

Although AuNPs synthesized are less competent compared to other systems, it provides an opportunity for water soluble and easy to synthesize AuNPs to be used as catalyst for various practical applications.

Similarly, by exploiting the competition between o-dianisidine and GSH for H_2O_2 the o-dianisidine- H_2O_2 -AuNPs system has again been used for GSH detection as given in Fig. 3.11 and Fig. 3.12. The pictorial representation in Fig. 3.10 indicates the change in color that occur due to increasing GSH concentration. The GSH competes for the H_2O_2 present in the system thus making less H_2O_2 available for o-dianisidine to react and form the colored product. Thus it can be concluded from the above study that the catalytic behavior of AuNPs is different from what it should have been on the basis of size of the nanoparticles, i.e., the smallest catalyzing the most, which is very well known from available literature (Haruta, 1997; Haruta, 2004; Hvolbaek et al., 2007). As the different shades of AuNPs that have been synthesized also differ in concentration of 3-APTMS used, the possibility of amine functionality assisted catalysis might be there. Accordingly, two different sizes of AuNPs (35 and 25 nm) were made keeping 3-APTMS concentration constant by varying the THF-HPO (11.3 mg, 33.9 mg) content. Fig. 3.13A and B show the results on GSH analysis and revealed that small size of AuNPs causes an increase in rate of catalysis which is in accordance with reported findings (Wang et al., 2009; Haruta, 1997; Haruta et al., 2004; Hvolbaek et al., 2007). Thus, the increased catalytic efficiency of AuNPs is a cumulative result of nanogeometry and functionality.

3.5. CONCLUSION

Novel findings on the controlled and rapid synthesis of AuNPs with size ranging from 10 nm to 40 nm based on the active participation of 3-APTMS and THF-HPO has been observed. An increase in the concentration of 3-APTMS increases the size of the AuNPs whereas an increase in THF-HPO concentration decreases the size of the same. Nanogeometry of as synthesized AuNPs can further be manipulated by addition of 3-APTMS even after the synthesis of the same. The flexibility in the synthesis technique allows formation of AuNPs of desired size at desired 3-APTMS and THF-HPO concentrations. The new process of AuNPs synthesis results in the conversion of THF-HPO to GBL which itself participates in nanoparticle formation under optimum concentration and forms imine derivatives of GBL with 3-APTMS. The as synthesized amine functionalized AuNPs also displays peroxidase mimetic behaviour and has an additional advantage as amine functionality assists the AuNPs in its catalyzing/sensing ability. The nanoparticles synthesized differ from other nanoparticles in its catalyzing ability that increases with increasing size, in conditions where both nanogeometry and functionality varies, which is attributed to the combined effect of nanogeometry and functionality. Although, when the effect of nanogeometry is studied alone by keeping amine functionality constant it shows the conventional behavior towards catalysis. Thus the synthesized AuNPs with tunable functionality and nanogeometry may be used for various applications in the future.